Integrated Multi-Resolution DEM Generation: Merging Airborne LiDAR and CartoDEM for Seamless Terrain Modeling

Runjhun Chandra, Anil Kumar G., Nalini J., Narender Bommineni

National Remote Sensing Centre, Hyderabad, India – runjhun_c@nrsc.gov.in, g_anilkumar@nrsc.gov.in, nalini_j@nrsc.gov.in, naren_br@nrsc.gov.in

Keywords: Digital Elevation Model (DEM), LiDAR, CartoDEM, Terrain Modeling, Geospatial Data Fusion.

Abstract

Accurate and continuous Digital Elevation Models (DEMs) are essential for hydrological modeling, terrain analysis, and large-scale geospatial planning. However, integrating elevation datasets from disparate sources—such as high-resolution airborne LiDAR and satellite-derived CartoDEM—requires careful handling of differences in spatial resolution and vertical accuracy. This study presents a structured workflow for generating integrated multi-resolution DEMs by merging airborne LiDAR data with CartoDEM products at 10 m and 30 m resolutions. The LiDAR point cloud was processed and resampled to a 30 m posting. Validated the quality of the derived DEMs with respect to 370 height control points, resulting in vertical RMSE of 1.5 m. For integration of different elevation datasets, a buffer-based blending approach was implemented using inverse distance weighting (IDW) interpolation across a 300 m transition zone, enabling smooth and gradual merging between the two datasets. This ensured the preservation of fine-scale terrain details from LiDAR while achieving seamless spatial continuity through CartoDEM support in peripheral regions. Quality checks were carried out using hillshade visualization and cross-sectional profile analysis across transition zones, ensuring no artefacts or elevation discontinuities persisted after merging. The final DEM maintains the fidelity of LiDAR-derived microtopography while leveraging CartoDEM for edge completeness and extended coverage. The workflow demonstrates a practical and scalable multi-resolution elevation model generation method, supporting broader geospatial initiatives and national mapping programs.

1. Introduction

High fidelity elevation data is crucial in geospatial applications such as hydrological modeling, terrain analysis, and floodplain delineation. High-resolution topographic datasets, especially those derived from airborne Light Detection and Ranging (LiDAR), are valued as they capture detailed surface variations and distinguish ground from non-ground features (Baltsavias, 1999). However, due to the high initial cost and limited extent of LiDAR surveys, it is often practical to supplement LiDAR DEM with open source medium-resolution DEMs, such as CartoDEM or SRTM-derived products, to achieve wider regional coverage.

In large-area studies—such as river basin modeling or infrastructure planning—high-resolution elevation data is typically restricted to zones of primary interest. However, the surrounding areas are filled with coarser elevation products. This multi-resolution approach is cost-effective, but it introduces data integration challenges. Merging datasets with differing resolutions and vertical accuracies can result in discontinuities, such as abrupt elevation steps, slope breaks, and hydrologically unrealistic transitions, if not handled carefully (Gallant, 2011; Okolie and Smit, 2022). Due to computation power of software/hardware being used to employ high resolution LiDAR DEMs, often there may be instances of users resampling the high resolution DEMs to coarser products, with improper resampling techniques, resulting in inconsistencies in the resampled product. This issue is also addressed in the study by generating multi resolution DEMs from LiDAR data itself and vertical accuracy of these resampled DEMs have been evaluated using control points.

Discrepancies at dataset boundaries arise from generalization between resolutions, datum inconsistencies, and systematic distortions. Several studies have attempted to mitigate these issues using blending or interpolation-based approaches. Standard techniques include inverse distance weighting (IDW), splines, or kernel-based methods applied over buffer zones to create smooth transitions (Huang et al., 2023). Meanwhile, recent advances in DEM fusion, such as weighted multi-source methods and sparse modelling, have demonstrated further potential to improve integration quality, particularly in complex terrains or under partial data availability (Fuse and Imose, 2023; Huang et al., 2023).

This study presents a two-part approach to address the challenge of multi-resolution DEM integration. First, LiDAR point cloud data (~1 pts/m^2) was processed to generate gridded raster DEMs at 10 m and 30 m resolutions. These resampled surfaces were evaluated for vertical accuracy using approximately 370 height control points distributed across diverse terrain, including flatlands, slopes, canals, forested regions, built-up areas. The validation process demonstrated that the resampled DEMs retained acceptable vertical accuracy levels and could be reliably used for regional analysis.

Following this, the second part of the study focused on merging the LiDAR-derived DEMs with CartoDEM data using a buffer-based blending approach. A 300-meter-wide transition zone was introduced between the datasets. This zone's elevation model was interpolated using IDW to ensure a smooth and continuous terrain surface. Visual validation using hillshade renderings and cross-sectional profiles were used to validate the final merged DEM. The merged DEM exhibited seamless integration, with no visible artefacts or topographic discontinuities.

The resulting integrated elevation model preserves the microtopographic detail of LiDAR in focus areas while extending spatial coverage using CartoDEM in peripheral regions. This scalable workflow supports a range of national and regional geospatial applications, particularly where continuous high-resolution data coverage is not available.

This contribution has been peer-reviewed. The double-blind peer-review was conducted on the basis of the full paper.
https://doi.org/10.5194/isprs-annals-X-5-W2-2025-77-2025 | © Author(s) 2025. CC BY 4.0 License.

2. Study Area and Data Used

The study focused on a major river basin in western India (Figure 1), comprising various land use and land cover classes, where coverage of Airborne Topographic LiDAR data was available. The following datasets were used for the study.

2.1 Airborne LiDAR Data

Airborne Laser Scanning (ALS) data used for this study was acquired using the Leica ALS70 sensor mounted on Beechcraft B200 aircraft platform, flown at 2,500 m height above ground level, collecting data in WGS84 datum. LiDAR point cloud has average point spacing of 1 points/m^2, with upto three returns per laser pulse. The collected point cloud was classified into ground and non-ground points using progressive densification algorithm. Using this classified data, Digital Elevation Models (DEMs) were generated and further resampled to 10 m and 30 m grid spacing (Figures 2 and 3).

2.2 CartoDEM

The coarser-resolution elevation data was sourced from CartoDEM Version 3.1 (Figure 4), generated from Cartosat-1 stereo imagery (Indian Space Reszearch Organisation, 2020). CartoDEM has a spatial resolution of 30 m and is referenced to the WGS84 horizontal datum with elevations relative to the WGS84 vertical datum. Updated 2.5m CartoDEM (National Remote Sensing Centre, 2024) was also used after resampling to 10m spacing, using bilinear interpolation.

Figure 1. Study Area for DEM Merging.

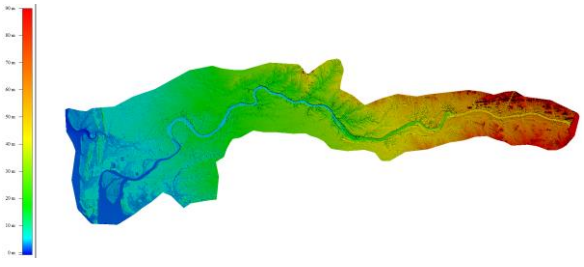

Figure 2. 10m DEM derived from LiDAR point cloud.

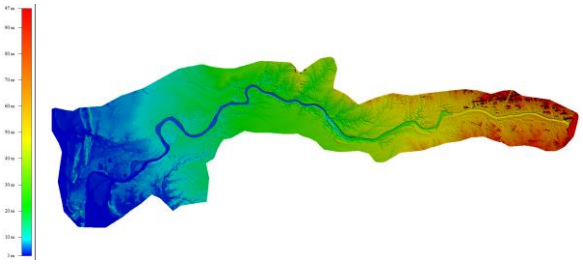

Figure 3. 30m DEM derived from LiDAR point cloud.

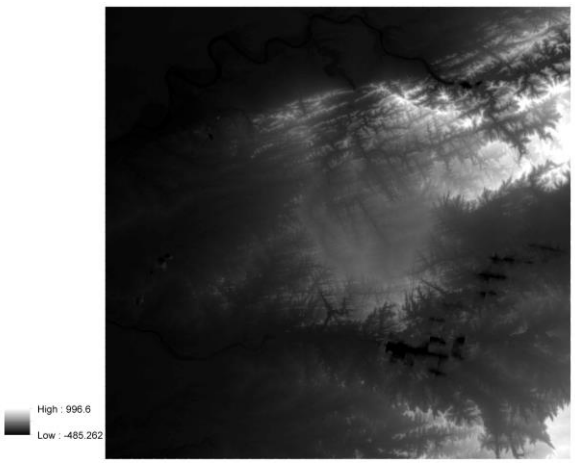

Figure 4. CartoDEM 30m product used for DEM merging.

3. Methodology

A structured workflow was adopted to generate an integrated Digital Elevation Model (DEM) by merging high resolution airborne LiDAR and coarse resolution CartoDEM datasets. The process was implemented for 10m as well as 30m spacing datasets to ensure smooth topographic transitions. The overall methodology is as follows.

Figure 5. Methodology for DEM Merging.

3.1 Pre-processing and Quality Check of LiDAR DEMs

The ground classified airborne LiDAR point cloud data and break-line data was processed to generate DEMs at 10 m and 30 m spatial resolutions. These resampled DEMs were derived from the LiDAR point cloud using triangulation, followed by spatial averaging to achieve the target grid resolutions. Parallelly, CartoDEM data derived from Cartosat-1 stereo imagery was utilized. The standard 30 m CartoDEM product was used directly, while the 2.5 m CartoDEM was resampled to 10 m resolution using bilinear interpolation to ensure compatibility across datasets. To maintain spatial consistency, all DEMs (LiDAR-derived and CartoDEM) were reprojected to the same standard spatial reference system: WGS84 UTM Zone 43N. Further, vertical accuracy of the LiDAR-derived DEMs was evaluated using approximately 370 control points (Figure 7) collected across diverse land cover types (refer to Figure 6 for workflow).

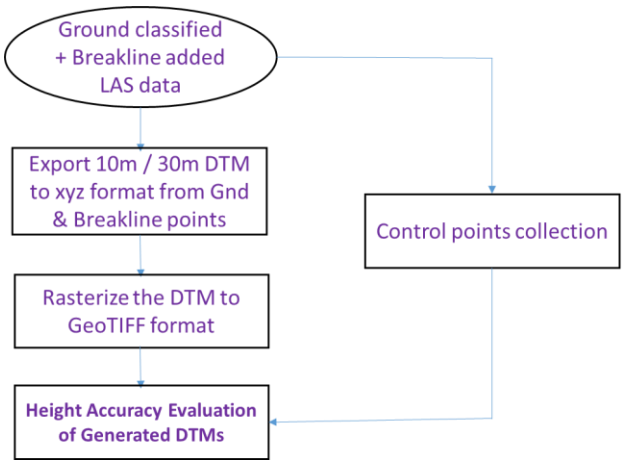

Figure 6. Workflow for Vertical Accuracy Evaluation.

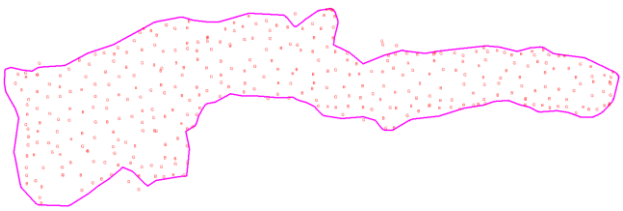

Figure 7. 370 control points collected in flat areas, river portions, slopes, canal portions, forest areas, and built-up areas.

The vertical Root Mean Square Error ($RMSE_Z$) was computed (Table 1) for both resolutions to confirm the suitability of down sampled LiDAR DEMs for further analysis.

Parameter	10m DEM	30m DEM
$Minimum_Z$	-6.57m	-9.02m
$Maximum_Z$	+1.59m	+3.79m
SD_Z	0.60m	1.11m
$RMSE_Z$	**0.62m**	**1.16m**

Table 1. Statistics for height differences between control points and DEMs at 10m and 30m spacing.

3.2 Co-Registration

Since the LiDAR-derived DEMs and CartoDEM products were referenced to the WGS84 datum (UTM Zone 43N projection) and exhibited no apparent horizontal or vertical shifts, no explicit co-registration was deemed necessary. As per ASPRS 2014 horizontal accuracy standards, spatial alignment within ±2.16 m (95% confidence) is acceptable for data intended for 1:5,000 scale mapping (ASPRS, 2014). The horizontal offsets observed between LiDAR-derived DEM and CartoDEM were consistently below this threshold, validating that no further co-registration was required. This compatibility allowed direct comparison and integration of the datasets without requiring further geometric transformation.

3.3 Identification of Transition Zone

To facilitate seamless merging, a 300-meter-wide buffer was delineated along the boundary of the LiDAR DEM coverage (Figure 8). The extent of the buffer was chosen using a trial and error method, starting with a 5 pixel zone in the 30m spacing datasets, extending up to 10 pixel (300m) wide zone. This buffer served as the transition zone where elevation blending between LiDAR and CartoDEM data will occur. The transition zone was defined spatially using vector operations and converted into raster format, aligned with the target resolution.

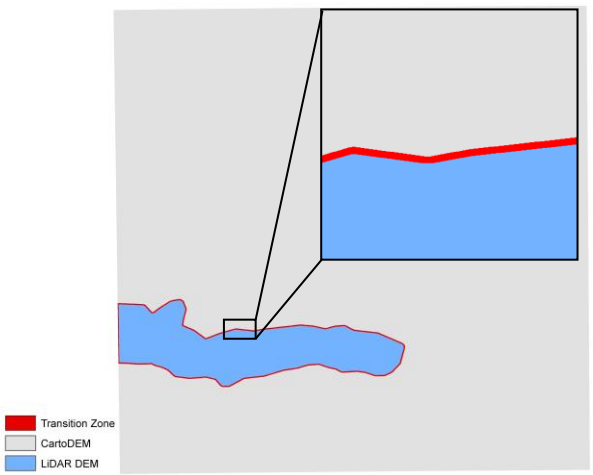

Figure 8. Extents of LiDAR DEM, CartoDEM, and Transition Zone, with a zoomed in view.

3.4 Blending

A localized adjustment surface was computed and applied within the defined transition zone to ensure a seamless transition between the high-accuracy LiDAR DEM and the less accurate CartoDEM. This blending process involved the following steps:

3.4.1 Computation of Elevation Difference: At the inner edge of the transition zone, where the LiDAR coverage ends, the elevation difference between the two DEMs was computed. This difference, denoted as H_diff, quantifies local mismatches arising due to differences in resolution, vertical accuracy, or terrain generalization. It served as the basis for calculating a smooth adjustment surface.

3.4.2 Preparation of Interpolation Input Points: Two sets of points were prepared as input for interpolation:

a) **Inner Edge Points**: Carried actual H_diff values, calculated by subtracting CartoDEM elevations from LiDAR DEM elevations.

a) **Outer Edge Points**: Assigned a zero value, representing the base CartoDEM surface.

Merging these point types into a single dataset ensured a gradient of elevation difference across the transition zone.

3.4.2 Surface Generation Using Interpolation: The merged point dataset was interpolated using the Inverse Distance Weighted (IDW) method to create a continuous difference (H_diff) surface. Each interpolated value Z(x) at location x is computed as:

$$Z(x,y) = \frac{\sum\left(\frac{Z_i}{d_i^p}\right)}{\sum\left(\frac{1}{d_i^p}\right)} \quad (1)$$

where Z(x, y) = interpolated value at the unknown point
Z_i = known value at point *i*
d_i = distance from the known point *i* to the interpolation point
p = power parameter
N = number of neighbors considered

Parameter tuning was performed to identify the most suitable configuration. A power value of 0.8 and 50 neighbors offered a smooth gradation while avoiding sharp breaks or artificial surface features.

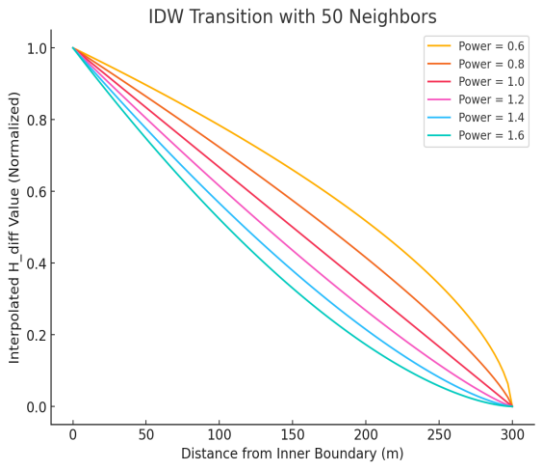

Figure 9. Profile comparison of IDW outputs for different power values.

3.4.3 Elevation Adjustment of CartoDEM: The interpolated difference surface was added to the CartoDEM within the transition zone. This adjustment allowed the CartoDEM values to progressively approach LiDAR elevations near the overlap boundary. Areas beyond the transition zone were not altered in either datasets.

3.4.4 Final DEM Merging: The final seamless DEM was constructed by combining three elevation layers- the original LiDAR DEM (retained within its valid spatial extent), the adjusted CartoDEM in the transition zone, and the unaltered CartoDEM outside this region. This integration was implemented using conditional raster algebra to ensure consistent coverage without duplication or gaps.

3.4.5 Post-Merge Validation: Visual and analytical checks were performed to verify the smoothness and quality of the merged DEM. A hillshade rendering (Figure 10) was generated to assess continuity, and elevation profiles were extracted across the transition zone. These helped confirm that no abrupt jumps or artefacts were introduced during blending.

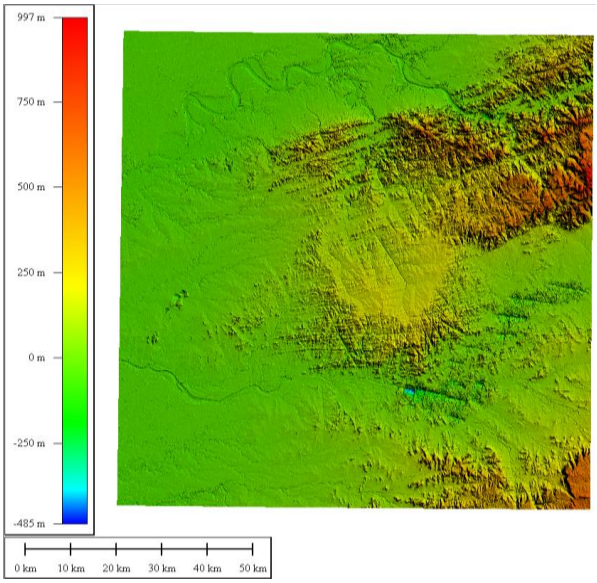

Figure 10. Hillshade view of the merged DEM.

This methodology ensured a smooth, artefact-free elevation model suitable for downstream applications such as hydrological simulations and large-area terrain analysis.

4. Results and Discussion

4.1 Visual Assessment of DEM Transition

Shaded relief visualization enhances surface features and allows intuitive assessment of the merged output. Before and after comparison is shown in Figure 11, clearly indicating the seamless transition in contrast to the sudden elevation change at the boundary. The resulting hillshade displayed a smooth and consistent terrain structure, with no visible breaks or distortions across the transition zone. This indicates that the IDW-based merging successfully preserved the surface characteristics and ensured seamless integration between datasets.

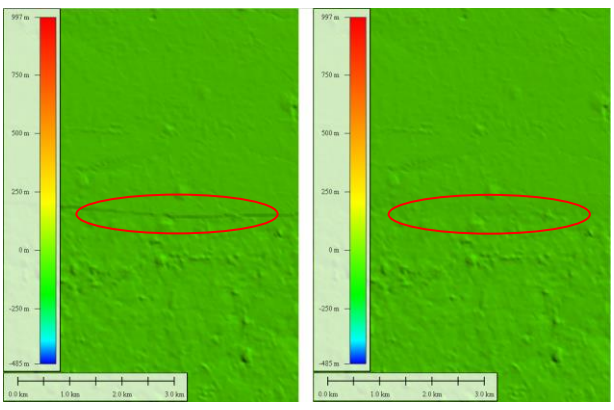

Figure 11. Hillshade view Before (left) and After (right).

4.2 Elevation Profile Comparison

For validating the merged DEM, ground truth information is required in the transition zone, to validate how well the interpolation has performed. To that end, another merged DEM, hereby referred to as validation DEM was generated, such that the entire transition zone falls within actual LiDAR coverage area. This ensured the availability of both actual elevation values (from LiDAR) and interpolated elevation values (from IDW blending). Four representative cross-sections were extracted from within the LiDAR region, from different terrain types, focusing on the transition zone, to compare actual and interpolated elevations (Figures 12 (a-d)). The comparison showed that the interpolated surface closely followed the LiDAR terrain, with deviations largely confined to within ±0.5 m. The smooth and gradual transition, with no abrupt changes or steps, further confirms the visual assessment.

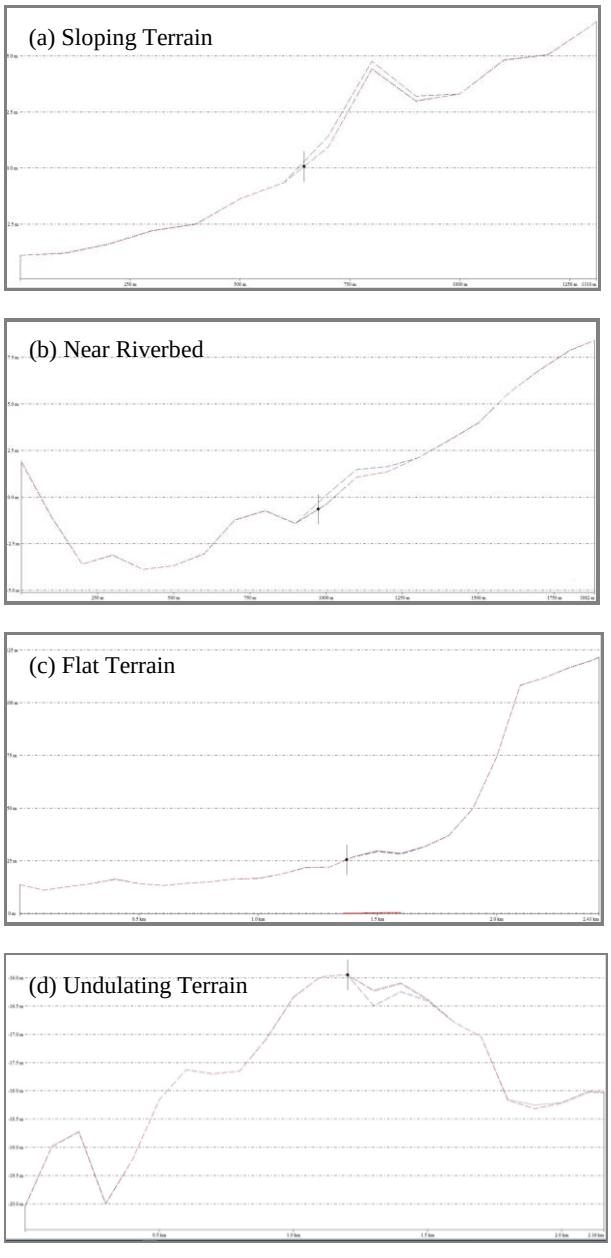

Figure 12. Cross-Sectional profiles in the transition zone (a-d). The Red dashed line represents LiDAR DEM, Blue dashed line represents Interpolated Surface (IDW).

4.3 Residual Analysis

The residual between the interpolated DEM and the LiDAR DEM was computed for the transition zone. No systematic bias was observed, indicating that IDW interpolation preserved the overall terrain shape.

4.4 Discussion on IDW Performance

The IDW method effectively preserved the LiDAR DEM's high-resolution features while ensuring a gradual transition to the coarser CartoDEM. The method offered high visual and numerical reliability without introducing artefacts such as domes or ridges (commonly associated with spline-based methods). Its ability to incorporate user-defined parameters such as power and number of neighbors allowed fine-tuning to suit the dataset characteristics. The blended DEM remains compatible with hydrological and terrain analysis workflows, such as watershed delineation and slope stability modeling, where continuity and accuracy are critical.

5. Conclusion

This study showcases a robust and scalable methodology for merging multi-resolution elevation datasets, specifically integrating high-resolution LiDAR-derived DEMs with the coarser CartoDEM using Inverse Distance Weighted (IDW) interpolation. The chosen IDW method ensured a smooth transition between the datasets, eliminating edge artefacts and retaining the vertical accuracy and surface detail of the LiDAR input. The merged DEM offers an enhanced and visually continuous terrain surface that overcomes the limitations of both individual sources.

Extensive quality checks, including visual inspection of hillshade surfaces and elevation profiles, confirmed the consistency and reliability of the merged output across varied terrain types. The resulting DEM is well-suited for hydrological modeling, flood simulation, and other geospatial analyses where resolution and regional continuity are essential.

The approach exhibits significant potential for large-scale terrain data enhancement by incorporating high-resolution datasets. Future work may explore integration with other global DEMs, automatic blending parameter optimization, and validation in application-specific contexts.

6. References

ASPRS, 2014. ASPRS Positional Accuracy Standards for Digital Geospatial Data. American Society for Photogrammetry and Remote Sensing. https://www.asprs.org/wp-content/uploads/2015/01/ASPRS_Positional_Accuracy_Standards_Edition1_Version100_November2014.pdf

Baltsavias, E.P., 1999. Airborne laser scanning: basic relations and formulas. *ISPRS Journal of Photogrammetry and Remote Sensing*, 54(2–3), pp.199–214.

Chukwuma J. Okolie, Julian L. Smit, 2022. A systematic review and meta-analysis of Digital elevation model (DEM) fusion: pre-processing, methods and applications, *ISPRS Journal of Photogrammetry and Remote Sensing*, Volume 188, Pages 1-29. https://doi.org/10.1016/j.isprsjprs.2022.03.016.

Dowling, T.I. & Gallant, J.C., 2003. A multi-resolution index of valley-bottom flatness for mapping depositional areas. *Water Resources Research*, 39(12), pp.1–13.

Fuse, T. & Imose, K., 2023. Comparative analysis of digital elevation model generation methods based on sparse modeling. *Remote Sensing*, 15(11), 2714. https://doi.org/10.3390/rs15112714

Gallant, J.C., 2019. Merging lidar with coarser DEMs for hydrodynamic modelling over large areas. In: *Proceedings of the 23rd International Congress on Modelling and Simulation (MODSIM)*, Canberra, Australia, pp.1161–1166. doi:10.36334/modsim.2019.K24.gallant

Höhle, J. & Höhle, M., 2009. Accuracy assessment of digital elevation models by means of robust statistical methods. *ISPRS Journal of Photogrammetry and Remote Sensing*, 64(4), pp.398–406.

Indian Space Research Organisation (ISRO), 2020. CartoDEM V3.1 – India's National Digital Elevation Model. National Remote Sensing Centre (NRSC), Hyderabad, India. https://www.nrsc.gov.in/sites/default/files/pdf/cartodem_bro_final.pdf

Huang, J., Wei, L., Chen, T., Luo, M., Yang, H. & Sang, Y., 2023. Evaluation of DEM accuracy improvement methods based on multi-source data fusion in typical gully areas of the Loess Plateau. *Sensors*, 23(8), 3878. https://doi.org/10.3390/s23083878

Indian Space Research Organisation (ISRO), 2020. *CartoDEM V3.1—India's national digital elevation model*. National Remote Sensing Centre (NRSC), Hyderabad.

Leitão, J.P., Prodanović, D. & Maksimović, Č., 2016. Improving merge methods for grid-based digital elevation models. *Computers & Geosciences*, 88, pp.115–131. https://doi.org/10.1016/j.cageo.2016.01.010

Li, J. & Heap, A.D., 2008. A review of spatial interpolation methods for environmental scientists. *Geoscience Australia Record*, 2008/23, Canberra, Australia.

National Remote Sensing Centre, 2024. *CartoDSM User Interface Manual (UIM 2024)*. Government of India, Bhoonidhi Portal.https://bhoonidhi.nrsc.gov.in/bhoonidhi_resources/help/UIM2024/9_UIM2024_CartoDSM.pdf

Rodriguez, F., Morris, E. & Belz, J., 2006. A global assessment of the SRTM performance. *Photogrammetric Engineering & Remote Sensing*, 72(3), pp.249–260.

Shepard, D., 1968. A two-dimensional interpolation function for irregularly spaced data. In: *Proceedings of the 1968 ACM National Conference*, New York, pp.517–524. https://doi.org/10.1145/800186.810616

Wehr, R. & Lohr, C., 1999. Airborne laser scanning—An introduction and overview. *ISPRS Journal of Photogrammetry and Remote Sensing*, 54(2), pp.68–82. https://doi.org/10.1016/S0924-2716(99)00011-8

Zhang, C. & Chen, S.C., 2021. A systematic evaluation of spatial interpolation methods for DEM generation from LiDAR point clouds. *Remote Sensing*, 13(6), 1132. https://doi.org/10.3390/rs13061132